Preliminary radiation dosimetry of a novel PET radiopharmaceutical ^{68}Ga-NODAGA-glycine in comparison with ^{99m}Tc-DTPA for renal studies

Mohsen Cheki[1] **MSc, PhD,**
Hariprasad Gali[2] **MSc, PhD**

1. Department of Radiologic Technology, Faculty of Paramedicine, Ahvaz Jundishapur University of Medical Sciences, Ahvaz, Iran
2. Department of Pharmaceutical Sciences, College of Pharmacy, the University of Oklahoma Health Sciences Center, Oklahoma City, OK, USA

Keywords: Gallium-68-NODAGA-glycine
- Medical internal radiation dose
- Renal agent
- Technetium-99m-diethylenetriamine pentaacetic acid

Corresponding author:
Mohsen Cheki, PhD
Department of Radiologic Technology,
Faculty of Paramedicine,
Ahvaz Jundishapur University of Medical Sciences,
Ahvaz, Iran
Tel/Fax: +98-9168186193
mohsencheky@gmail.com

Received:
25 October 2017
Accepted revised:
20 November 2017

Abstract

Objective: In this study, we tried to estimate human absorbed dose of ^{68}Ga-NODAGA-glycine as a new potential positron emission tomography (PET) renal agent based on the biodistribution data reported in healthy rats, and compare our estimation with the available absorbed dose data from technetium-99m-diethylenetriaminepentaacetic acid (^{99m}Tc-DTPA). **Subjects and Methods:** The medical internal radiation dose (MIRD) formulation was applied to extrapolate from rats to human and to project the absorbed radiation dose for various organs in humans. S factor calculated by Monte-Carlo N-particle (MCNP) simulation and also this factor has been taken from the tables presented in MIRD pamphlet No.11. Hence, two radiation absorbed dose were calculated for organs. **Results:** Our dose prediction shows that an 185MBq injection of gallium-68-1,4,7-triazacyclononane-1--glutamylglycine-4,7-diacetic acid (^{68}Ga-NODAGA-glycine) in humans might result in an estimated absorbed dose of 0.063mGy in the whole body when S factor calculated by MCNP simulation. The highest absorbed doses are observed in kidneys, lungs, spleen, liver, and red marrow with 3.510, 0.453, 0.335, 0.268, and 0.239mGy, respectively. In addition to, the estimated absorbed dose for total body after injection of 185MBq of ^{68}Ga-NODAGA-glycine is 0.053mGy when S factor has been taken from MIRD pamphlet No.11. The highest absorbed doses are observed in kidneys, lungs, liver, spleen, and red marrow with 3.110, 0.438, 0.209, 0.203, and 0.203mGy, respectively. Comparison between human absorbed dose estimation for ^{68}Ga-NODAGA-glycine and ^{99m}Tc-DTPA indicated that the absorbed dose of the most organs after injection of ^{99m}Tc-DTPA is higher than the amount after ^{68}Ga-NODAGA-glycine. **Conclusion:** The results showed that ^{68}Ga-NODAGA-glycine delivers lower dose to the patients. Also due to its application in PET (which offers higher sensitivity and spatial resolution compared to planar or SPET), ^{68}Ga-NODAGA-glycine would be a superior choice than ^{99m}Tc-DTPA for renography and impose less radiation doses to patients.

Hell J Nucl Med 2017; 20(3): 241-246 *Published online: 11 December 2017*

Introduction

A radiation dose assessment, i.e., calculations of the absorbed and effective doses per unit activity administered is mandatory for the translation of novel radiotracers from preclinical to clinical study phases [1, 2]. Also, the Food and Drug Administration (FDA) studies a number of safety issues during the drug approval process, and internal dosimetry is one issue of high importance [3]. A high radiation dose to vital organs may prevent the use of an imaging agent [4].

Dosimetric evaluations perform mainly with the medical internal radiation dose (MIRD) method. This method is based on knowledge of the cumulated activity in an organ or tissue (source), and the absorbed fraction of energy in the organ or tissue of interest (target) due to radiation emitted by the source. Thus, the absorbed dose to the target is obtained by summing up the contributions from all source regions [5-7].

Techentium-99m-diethylenetriamine pentaacetic acid (^{99m}Tc-DTPA) based planar gamma-imaging remain the nuclear imaging techniques of choice for the clinical evaluation of renal function and renography [8-10]. Although renography provides important information about the renal function that helps in the diagnosis and management of patients with suspected renal and urinary tract problems, there are drawbacks associated with the use of the planar imaging technique. Clinical positron emission tomography (PET) cameras offer higher sensitivity, spatial resolution, and signal-to-noise ratios than clinical gamma/single-photon emission tomography (SPET) cameras. For example, spatial resolution of a clinical PET camera and a clinical gamma/SPET camera is 4-6mm and 10-20mm, respectively [11, 12]. Hence, there is a need to develop suitable radiotracers to utilize PET in clinical evaluation of renal function. Gallium-68 (^{68}Ga) as an excellent PET radionuclide has

stimulated researchers to investigate the potential of ^{68}Ga-based PET imaging agents. Gallium-68 has very special physical characteristics [positron emission (89%), low abundance of 1077keV photon emission (3.22%), and the relatively short half-life ($t_{1/2}$=67.71min)] [13, 14]. Recently, ^{68}Ga-NODAGA-glycine was identified as a potential PET renal agent [12]. ^{68}Ga-NODAGA-glycine can be obtained by a single step labeling procedure by reacting NODAGA-glycine with $^{68}GaCl_4^-$ (eluted from a ^{68}Ge/^{68}Ga generator) at room temperature for 10min [12]. NODAGA-glycine is synthesized from commercially available 4-(4,7-bis(2-(tert-butoxy)-2-oxoethyl)-1,4,7-triazacyclononan-1-yl)-5-(tert-butoxy)-5-oxopentanoic acid (NODA-GA(tBu)$_3$) [12]. Gallium-68-NODAGA-glycine demonstrated fast and exclusive clearance through the renal-urinary pathway with 0.50±0.08 and 0.06±0.01 %ID/g remained in blood at 10min and 1hr post-injection respectively [12]. Also, it was not taken up by any extra-renal tissue and displayed no activity retention in the kidneys [12]. Positron emission tomography renography conducted in healthy rats with ^{68}Ga-NODAGA-glycine revealed time-to-peak (T_{max}) and time to half-maximal activity ($T_{1/2max}$) values of 5.8±2.3min and >15min respectively [12]. Additionally, ^{68}Ga-NODAGA-Glycine PET renography provided high quality PET/CT images (Figure 1). In vivo biodistribution of ^{68}Ga-NODAGA-glycine in healthy rats is known, but its radiation absorbed dose is not yet known. Thus, the present study attempts to estimate the absorbed dose of ^{68}Ga-NODAGA-glycine in human based on biodistribution data reported in healthy rats and compare our data with available absorbed dose data from ^{99m}Tc-DTPA, as documented in the International Commission on Radiological Protection (ICRP) publication 80.

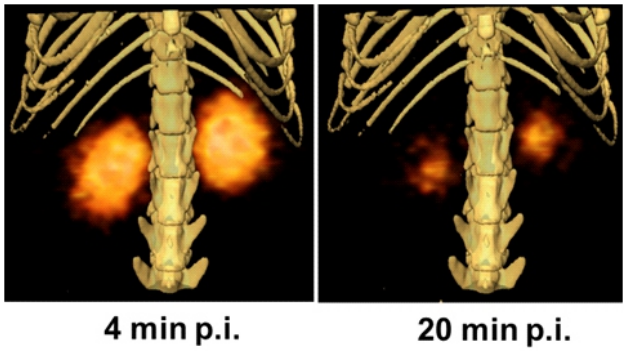

Figure 1. Abdominal PET/CT images (maximum intensity projection) of a healthy female Sprague-Dawley rat injected with ^{68}Ga-NODAGA-Glycine (3.7MBq) [12].

Subjects and Methods

The biodistribution data of ^{68}Ga-NODAGA-glycine in various organs of a healthy rat as a percentage of the injected dose per gram tissue (%ID/g) at 10min and 60min post-injection was taken from previously reported study [12]. Briefly, two groups (n=5) of healthy female Sprague Dawley rats of weight 236-286g were anesthetized and injected with a dose of ^{68}Ga-NODAGA-glycine (~3.3MBq) in normal saline (0.2mL) through a tail vein catheter, followed by 0.5mL of saline [12]. Rats were kept under anesthesia during the study and were eutha-nized at 10min or 1h post-injection. The tissues/organs were excised, weighed, and the radioactivity associated with each sample was measured using an automated gamma counter. The radioactivity counts were background and decay corrected. The radioactivity uptake expressed as injected dose per gram (%ID/g) for each tissue/organ was then calculated [12].

Extrapolation of the animal organ uptake data to humans

In this study, the organ uptake data in animals were extrapolated to the equivalent uptake in humans by the proposed method of Sparks et al. (1996) [15] as represented in Equation 1:

$$(\%ID/g)_{human} = [(\%ID/g)_{animal} \times (kg_{TBweight})_{animal}] \times \left(\frac{g_{organ}}{kg_{TBweight}}\right)_{human} \quad (1)$$

where $(\%ID_{organ})_{human}$ denotes the percentage of injected activity in a human organ, $(kg_{TBweight})_{animal}$ is the body we-ight of the rat, and $(g_{organ}/kg_{TBweight})_{human}$ is the ratio bet-ween the weights of human organ and human body. The mean weight of the organs harvested from the animals and the standard weights established for the adult male human organs were used [16-18].

Cumulated activity calculations

The cumulated activity in the source organs, $\tilde{A}_h$ can be calculated by the equation 2 [19]:

$$\tilde{A} = \int_{t1}^{\infty} A(t)dt \quad (2)$$

where Ã (t) is the activity of each organ at the time t. In this study, the accumulated source activity was calculated by plotting the non-decay-corrected time activity curves for each organ and computing the area under the curves. For this purpose, the data points which represented the percentage-injected dose were created and fitted to a mono-exponential or to an uptake and clearance curve by MATLAB software (Version. 7.5). In addition, the curves were extrapolated to infinity by fitting the tail of each curve to a monoexponential curve. Then, the area under the curve was calculated as described previously by Shanehsazzadeh et al. (2009) [20]. To prevent under-sampling for the area under the curves (AUC), we tried to calculate the AUC when the R^2 square of fitted curves was above 0.9 for each organ.

Absorbed dose calculations

The absorbed dose was calculated by MIRD formulation [21]:

$$D_{r_k} = \sum_h \tilde{A}_h \times S(r_k \leftarrow r_h) \quad (3)$$

where $D(r_k)$ is the absorbed dose in the target organ, $\tilde{A}_h$ is the cumulated activity in source organs and $S(r_k \leftarrow r_h)$ called S factor is defined as the mean absorbed dose to the target

region r_k per unit cumulated activity in the source region r_h. S Factor represents the physical decay characteristics of the radionuclide, the range of the emitted radiations, and the organ size and configuration expressed in mGy (MBq s)$^{-1}$. In this study, the S factors were calculated by Monte-Carlo N-particle (MCNP) simulation and this factor has been taken also from the tables presented in MIRD pamphlet No.11 [17].

Calculations of S factor by MCNP simulation

In this study, the MIRD mathematical phantom was used as an input for Monte Carlo calculations of S factors for ^{68}Ga by using the MCNPX 2.6c code. The mathematical phantom is a representation of the human body. In these phantoms, all organs are represented with geometrical bodies (such as cylinders, ellipsoids, tori etc), which are described with suitable mathematical equations. A corresponding chemical constitution for various types of organ tissues is also defined [22]. It was assumed that ^{68}Ga was uniformly distributed within the specified source organs with isotropic direction emission. Major organs were chosen to be both the source and the target while the others were set as targets only. Electron and photon energies as well as the probability for emission for ^{68}Ga were extracted from the RADDECAY v3 software (Charles Hacker, Griffith University, Gold Coast, Australia). This program uses data from Radiation Shielding Information Center (RSIC) at Oak Ridge National Laboratories (USA), whereas the energy spectra for the beta-particles were obtained from the RADAR website [23]. To calculate the S values, each source organ required individual simulation. To maintain the statistical error of the simulations below 1%, 50×10^6 source particles were simulated. All simulations were performed on a 96 nodes Linux cluster using a 64-bit compiled version of the MCNPX 2.6c code. To calculate the energy deposited in the target sources, the $*F8$ tally was set for each target. An $*F8$ tally gives the energy deposition in MeV per primary particle. The S-factor was calculated as follows [24]:

$$S\left(r_k \leftarrow r_h\right) = 1.6 \times 10^{-10} \frac{\sum_{part} \sum_i (*F8)_i . n_i}{M_t} \quad (4)$$

where $(*F8)_i$ is the energy deposited from particles emitted with energy E_i in the target organ t-in MeV-as obtained from MCNP4c2, and n_i is the number of particles per decay for the particles of energy E_i. The $(*F8)_i \cdot n_i$ values were summed for all emissions (photons and electrons) and divided by the mass of the target organ M_t in g. The factor 1.6×10^{-10} was used to obtain the S-factor values in Gy Bq^{-1} s^{-1}.

Calculation of effective dose

The effective dose of each organ was concluded by the equation 5:

$$E = \sum_T H_T \times w_T \quad (5)$$

$$H_T = \sum_T D_{T,R} \times w_R$$

where H_T is the equivalent dose in a tissue or organ. $D_{T,R}$ is the absorbed dose in tissue T by radiation type R and w_R is the radiation weighting factor, w_T is the tissue-weighting factor according to ICRP publication 103 [25].

Results

The radiation absorbed dose of organs estimated in humans according to the rats data are presented in Table 1. The amount of the absorbed dose to a human was calculated by multiplying the converted rats' cumulative activity (using relative organ mass extrapolation) to the S factor. S factor calculated by MCNP simulation and also this factor has been taken from the tables presented in MIRD pamphlet No.11. Hence, two absorbed dose are shown in Table 1 for organs.

The estimated absorbed dose for total body after injection of 185MBq of ^{68}Ga-NODAGA-glycine was 0.063mGy when S factor calculated by MCNP simulation. The highest absorbed dose is observed in the kidneys with 3.510mGy, and the organs that received the next higher dose were lungs, spleen, liver, and red marrow with the magnitude of 0.453, 0.335, 0.268, and 0.239mGy, respectively. Furthermore, the estimated absorbed dose for total body after injection of 185MBq of ^{68}Ga-NODAGA-glycine was 0.053mGy when S factor has been taken from MIRD pamphlet No.11. The highest absorbed dose was observed in the kidneys with 3.110mGy, and the organs that received the next higher dose were lungs, liver, spleen, and red marrow with the magnitude of 0.438, 0.209, 0.203, and 0.203mGy, respectively. As demonstrated in Table 1, our estimation shows that all organs received doses when S factor calculated by MCNP simulation in comparison with when S factor had been taken from MIRD pamphlet No.11. On the other hand, as documented in ICRP 80 [26], the total body absorbed dose after injection of 185MBq of ^{99m}Tc-DTPA was 1.517mGy. The highest absorbed dose was observed in the bladder wall with 14.245mGy, and the organs, which received the next higher dose were uterus, kidneys, lower large intestine (LLI) wall, and ovaries with the amount of 1.850, 1.054, 1.036, and 1.017mGy, respectively. This discrepancy between our MCNP simulation and MIRD pamphlet No.11 could be attributed to the different in simulation assumptions. In MIRD pamphlet No. 11, the absorbed fraction (AF) is considered zero for electrons and beta particles, unless target organ and source organ are the same, in which case AF is 1. The same holds true for X-rays or γ-radiation with energies less than 10keV in MIRD pamphlet No. 11. These assumptions are not considered in this study.

The comparison of our estimation of human absorbed dose of ^{68}Ga-NODAGA-glycine with ^{99m}Tc-DTPA in accordance with ICRP 80 [26] is depicted in Figure 1. As demonstrated in Figure 2, our estimation showed that all of the organs, except kidneys and lungs received higher doses when ^{99m}Tc-DTPA was prescribed in comparison with ^{68}Ga-NODAGA-glycine.

Discussion

Table 1. *Estimation of human absorbed doses from rat data after intravenous administration of ^{68}Ga-NODAGA-glycine.*

Target organs[a]	Absorbed dose (mGy/MBq)[b]	Absorbed dose (mGy/MBq)[c]	Absorbed dose (mGy)[b,1]	Absorbed dose (mGy)[c,1]	W_T [d]	Effective absorbed dose (mSv)[b,1]	Effective absorbed dose (mSv)[c,1]
Kidneys	1.68E-02	1.90E-02	3.11E+00	3.51E+00	0.12	3.73E-01	4.22E-01
Liver	1.13E-03	1.45E-03	2.09E-01	2.68E-01	0.04	8.36E-03	1.07E-02
Red marrow	1.10E-03	1.29E-03	2.03E-01	2.39E-01	0.12	2.44E-02	2.86E-02
Lungs	2.37E-03	2.45E-03	4.38E-01	4.53E-01	0.12	5.26E-02	5.44E-02
Spleen	1.10E-03	1.81E-03	2.03E-01	3.35E-01	0.12	2.44E-02	4.02E-02
Muscle	1.22E-04	1.34E-04	2.26E-02	2.48E-02	0.12	2.71E-03	2.97E-03
ULI wall	5.90E-04	6.09E-04	1.09E-01	1.13E-01	0.12	1.31E-02	1.35E-02
LLI wall	7.43E-04	8.01E-04	1.37E-01	1.48E-01	0.12	1.65E-02	1.78E-02
Stomach wall	4.17E-04	4.68E-04	7.71E-02	8.66E-02	0.12	9.26E-03	1.04E-02
SI	9.44E-04	10.55E-04	1.75E-01	1.95E-01	0.12	2.10E-02	2.34E-02
Uterus	6.73E-05	7.20E-05	1.24E-02	1.33E-02	0.12	1.49E-03	1.60E-03
Adrenals	3.52E-04	4.33E-04	6.51E-02	8.01E-02	0.12	7.81E-03	9.61E-03
Testes	2.81E-06	3.74E-06	5.20E-04	6.92E-04	0.08	4.16E-05	5.53E-05
Bladder wall	4.27E-05	4.87E-05	7.90E-03	9.01E-03	0.04	3.16E-04	3.60E-04
Thyroid	3.80E-05	4.19E-05	7.03E-03	7.75E-03	0.04	2.81E-04	3.10E-04
Pancreas	2.42E-04	2.77E-04	4.48E-02	5.12E-02	0.12	5.37E-03	6.15E-03
Ovaries	1.31E-05	1.95E-05	2.42E-03	3.61E-03	0.08	1.94E-04	2.89E-04
Skin	4.41E-05	4.69E-05	8.16E-03	8.68E-03	0.01	8.16E-05	8.68E-05
Total body	2.89E-04	3.43E-04	5.35E-02	6.35E-02	1	5.35E-02	6.35E-02

[a]LLI; lower large intestine, ULI; upper large intestine, SI; small intestine. [b]S factors have been taken from MIRD pamphlet No.11 for calculations of absorbed dose and effective absorbed dose. [c]S factors calculated by MCNP simulation for calculations of absorbed dose and effective absorbed dose.

[d]Tissue weighting factors according to International Commission on Radiological Protection ICRP103 (ICRP2007) [25].

[1]If injected 185MBq activity of radiotracer.

The extrapolation of animal data to humans is far from an exact procedure. However, according to ICRP 62 recommendations, results from such studies represent an important first step in the evaluation of radiation dose, before moving forward to human measurements from a small number of volunteers [27]. Also, several studies have demonstrated the usefulness of using animal distribution as a model for absorbed dose estimations in humans [28-30].

In this study, we predict and compare the absorbed dose from ^{68}Ga-NODAGA-glycine and ^{99m}Tc-DTPA. Galium-68 gamma rays with 511keV and higher energies have lower cross section to the neighbor organs and therefore lower dose deliveries occur [14]. As represented in Figure 2, ^{99m}Tc-DTPA delivers higher doses compared to ^{68}Ga-NODAGA-glycine. The kidneys and lung received to times higher dose when ^{68}Ga-NODAGA-glycine was injected compared to ^{99m}Tc-DTPA. This condition was in reverse order for other organs. Our prediction and documented data from ICRP showed that the absorbed dose ratios for ^{99m}Tc-DTPA/^{68}Ga-NODAGA-glycine in the other organs such as ovaries, thyroid, pancreas, adrenals, red marrow, and liver were about 282.05, 35.79, 7.58, 4.61, 1.70, and 1.24, respectively. These results

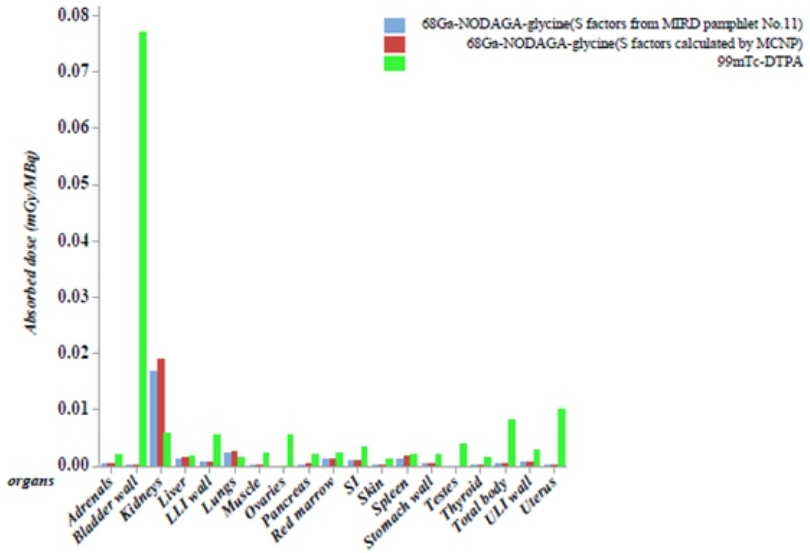

Figure 2. Comparison between our estimation of radiation absorbed dose for ^{68}Ga NODAGA-glycine versus data from ^{99m}Tc-DTPA in humans based on ICRP 80 data [26].

are in accordance with previous results, which compared ^{68}Ga vs ^{99m}Tc, ^{111}In vs. ^{68}Ga and ^{68}Ga vs ^{67}Ga [14, 31, 32]. One of our limitations in this study is that we compare our estimated absorbed dose from ^{68}Ga-NODAGA-glycine with the real value data derived from ICRP 80 [26].

According to title 21 of the Code of Federal Regulations (21 CFR 361.1) [33], the radiation dose to the whole body, active blood-forming organs, lens of the eye, and gonads cannot be more than 3rem (30mSv) in a single study, and a total of greater than 5rem (50mSv) per year during the entire study. For all other organs, the limits are 5rem (50mSv) per single study and 15rem (150mSv) annually. As shown in Table 1 all organs received less than the permitted absorbed dose which is a good factor to use this radiopharmaceutical. Also, our prediction indicated that the absorbed dose to these organs did not exceed the threshold dose, consistent with ALARA law.

Planar imaging provides limited structural information, low-quality images, and poor quantitative data. These drawbacks could be overcome by using a tomographic imaging technique such as SPET or PET. However, conducting a clinical dynamic SPET study is technically challenging. The clinical SPET camera depends on rotational movement (step-and-shoot) of detector heads, which cannot be used for renography due to fast pharmacokinetics exhibited by the renal agents used. Positron emission tomography overcomes these technical challenges and enables the use of tomographic imaging for renography and also uses a series of detector blocks arranged in a cylindrical geometry around the subject, which allows acquisition of imaging data with high temporal and spatial resolutions. In addition, clinical PET provides substantially superior quantitative data and also better structural information due to high sensitivity, spatial resolution and signal-to-noise ratios than SPET cameras [11, 34]. Thus, the higher amount of radiation dose for kidneys and lungs can be lowered by a lower prescribed dose of ^{68}Ga-NODAGA-glycine.

In conclusion, in this study, comparison between human absorbed dose estimation for these two renal imaging agents indicated that the absorbed dose of the most organs, except for kidneys and lungs, after injection of ^{68}Ga-NODAGA-glycine was lower than the amount after ^{99m}Tc-DTPA injection. Also, ^{99m}Tc-DTPA to ^{68}Ga-NODAGA-glycine total body absorbed dose ratio was nearly equal to 24. Furthermore, the ^{99m}Tc-DTPA remains longer than ^{68}Ga-NODAGA-glycine in kidneys and lungs, and ^{68}Ga-NODAGA-glycine requires injecting lower dose. Our results suggest that ^{68}Ga-NODAGA-glycine delivers a lower dose to the patients and by using PET study may be a better candidate for imaging the kidneys giving less radiation doses to patients compared to ^{99m}Tc-DTPA.

This research was supported by grants (U-96091) from the vice chancellor of research at Ahvaz Jundishapur University of Medical Sciences (Iran).

The authors of this study declare no conflicts of interest

Bibliography

1. Sakata M, Oda K, Toyohara J et al. Direct comparison of radiation dosimetry of six PET tracers using human whole-body imaging and murine biodistribution studies. *Ann Nucl Med* 2013; 27: 285-96.
2. Kawamura K, Ishiwata K, Shimada Y et al. Preclinical evaluation of [^{11}C]SA4503: radiation dosimetry, in vivo selectivity and PET imaging of sigma1 receptors in the cat brain. *Ann Nucl Med* 2000; 14: 285-92.
3. Eberlein U, Bröer JH, Vandevoorde C et al. Biokinetics and dosimetry of commonly used radiopharmaceuticals in diagnostic nuclear medicine-a review. *Eur J Nucl Med Mol Imaging* 2011; 38: 2269-81.
4. Velikyan I, Rosenström U, Bulenga TN et al. Feasibility of multiple examinations using ^{68}Ga-Labelled collagelin analogues: organ distribution in rat for extrapolation to human organ and whole-body radiation dosimetry. *Pharmaceuticals (Basel)* 2016; 9: 31.
5. Mattsson S. Patient dosimetry in nuclear medicine. *Radiat Prot Dosimetry* 2015; 165: 416-23.

6. Cheki M, Shahbazi Gahrouei D, Moslehi M. Determination of organ absorbed doses in patients following bone scan with using of MIRD method. *Iran South Med J* 2013; 16: 296-303.
7. Shahbazi-Gahrouei D, Cheki M, Moslehi M. Estimation of organ absorbed doses in patients from ^{99m}Tc-diphosphonate using the data of MIRDose software. *J Med Signals Sens* 2012; 2: 231-4.
8. Gates G. Glomerular filtration rate: estimation from fractional renal accumulation of ^{99m}Tc-DTPA (stannous). *AJR* 1982; 138: 565-70.
9. Barbour GL, Crumb CK, Boyd CM et al. Comparison of inulin, iothalamate, and ^{99m}Tc-DTPA for measurement of glomerular filtration rate. *J Nucl Med* 1976; 17: 317-20.
10. Hadzhiyska V, Kostadinova I, Demirev A. Is there an advantage in performing a combined examination: diuretic renal scintigraphy and low dose computed tomography compared to the separate use of these methods in urolithiasis. *Hell J Nucl Med* 2015; 18: 90-2.
11. Townsend DW. Positron emission tomography/computed tomography. *Semin Nucl Med* 2008; 38: 152-66.
12. Pathuri G, Hedrick AF, January SE et al. Synthesis and in vivo evaluation of gallium-68-labeled glycine and hippurate conjugates for positron emission tomography renography. *J Labelled Comp Radiopharm* 2015; 58: 9-14.
13. Yang DJ, Kim EE, Inoue T. Targeted molecular imaging in oncology. *Ann Nucl Med* 2006; 20: 1-11.
14. Shanehsazzadeh S, Yousefnia H, Jalilian A et al. Estimated human absorbed dose for ^{68}Ga-ECC based on mice data: comparison with ^{67}Ga-ECC. *Ann Nucl Med* 2015; 29: 475-81.
15. Sparks RB, Aydogan B. Comparison of the effectiveness of some common animal data scaling techniques in estimating human radiation dose. Sixth international radiopharmaceutical dosimetry symposium Oak Ridge. *Oak Ridge Associated Universities* 1996; 2: 705-16.
16. ICRP. Radiation dose to patients from radiopharmaceuticals. Addendum 3 to ICRP Publication 53. ICRP Publication 106. Approved by the Commission in October 2007. *Ann ICRP* 2008; 38: 1-197.
17. Snyder WS, Ford MR, Warner GG et al. "S", absorbed dose per unit cumulated activity for selected radionuclides and organs. *MIRD Pamphlet No. 11*. New York: Society of Nuclear Medicine; 1975; 1-258.
18. Keenan MA, Stabin MG, Segars WP et al. RADAR realistic animal model series for dose assessment. *J Nucl Med* 2010; 51: 471-6.
19. Bevelacqua JJ. Internal Dosimetry Primer. *Radiat Prot Manage* 2005; 22: 7-17.
20. Shanehsazzadeh S, Jalilian AR, Sadeghi HR et al. Determination of human absorbed dose of ^{67}GA-DTPA-ACTH based on distribution data in rats. *Radiat Prot Dosim* 2009; 134: 79-86.
21. Stabin MG, Siegel JA. Physical models and dose factors for use in internal dose assessment. *Health Phys* 2003; 85: 294-310.
22. Shahbazi-Gahrouei D, Ayat S. Determination of organ doses in radioiodine therapy using monte carlo simulation. *World J Nucl Med* 2015; 14: 16-8.
23. Stabin MG, da Luz LC. Decay data for internal and external dose assessment. *Health Phys* 2002; 83: 471-5.
24. Bitar A, Lisbona A, Thedrez P et al. A voxel-based mouse for internal dose calculations using Monte Carlo simulations (MCNP). *Phys Med Biol* 2007; 52: 1013-25.
25. ICRP. Recommendations of the International Commission on Radiological Protection. ICRP Publication 103. *Ann ICRP* 2007; 37: 1-332.
26. ICRP. Radiation Dose to Patients from Radiopharmaceuticals. Addendum to ICRP Publication 53. ICRP Publication 80. *Ann ICRP* 1998; 28: 1-85.
27. ICRP. Radiological protection in biomedical research. ICRP Publication 62. *Ann of ICRP* 1992; 22.
28. Constantinescu CC, Garcia A, Mirbolooki MR et al. Evaluation of [^{18}F]Nicene biodistribution and dosimetry based on whole-body PET imaging of mice. *Nucl Med Biol* 2013; 40: 289-94.
29. Bélanger MJ, Krause SM, Ryan C et al. Biodistribution and radiation dosimetry of [^{18}F]F-PEB in nonhuman primates. *Nucl Med Com-mun* 2008; 29: 915-9.
30. Kesner AL, Hsueh WA, Czernin J et al. Radiation dose estimates for [^{18}F]5-fluorouracil derived from PET-based and tissue-based methods in rats. *Mol Imaging Biol* 2008; 10: 341-8.
31. Shanehsazzadeh S, Lahooti A, Yousefnia H et al. Comparison of estimated human dose of ^{68}Ga-MAA with ^{99m}Tc-MAA based on rat data. *Ann Nucl Med* 2015; 29: 745-53.
32. Wild D, Wicki A, Mansi R et al. Exendin-4-based radiopharmaceuticals for glucagonlike peptide-1 receptor PET/CT and SPECT/CT. *J Nucl Med* 2010; 51: 1059-67.
33. Food and Drug Administration. Title 21 CFR 361.1, Radioactive Drugs for Certain Research Uses. In 4-1-01 ed; National Archives and Records Administration, Washington, 2001; p 300-5.
34. Nkepang GN, Hedrick AF, Awasthi V et al. Facile synthesis of para-[^{18}F]fluorohippurate via iodonium ylide-mediated radiofluorination for PET renography. *Bioorg Med Chem Lett* 2016; 26: 479-83.